Geological Quarterly, 2008, 52 (4): 369–382

Comparative study on the Late Cenozoic red clay deposits from China and Central Europe (Hungary)

János KOVÁCS, György VARGA and József DEZSŐ

Kovács J., Varga G. and Dezső J. (2008) — Comparative study on the Late Cenozoic red clay sediments from China and Central Europe (Hungary). Geol. Quart., **52** (4): 369–382. Warszawa.

In the eastern Loess Plateau region of Northern China, the Quaternary loess-palaeosol sequences of the last 2.6 Ma are underlain by the *Hipparion* Red-Earth Formation (namely the "Red Clay"). The red clay is also a significant deposit in Hungary, the origin of which is controversial. This paper is a comparative study of the Central European (Hungarian) red clay succession and the Xifeng Red Clay profile, the type section for this deposits in the eastern Loess Plateau region. Optical microscopic and SEM analysis were used for grain-size measurements, and both major- and trace-element geochemical properties were analysed to address the question of the origin of Hungarian red clay as well as its environmental implication. We compare the Xifeng Upper Red-Earth (age: ~3.6 to 2.6 Ma BP) with the Hungarian, Tengelic Red Clay Formation (age: ~3.5 to 1.0 Ma BP); both are aeolian deposits genetically related to the Quaternary loess-palaeosol sequence.

János Kovács, György Varga, Department of Geology, University of Pécs, Ifjúság u. 6, H-7624 Pécs, Hungary; e-mails: jones@gamma.ttk.pte.hu, gyoker@gamma.ttk.pte.hu; József Dezső, Institute of Environmental Sciences, University of Pécs, Ifjúság u. 6, H-7624 Pécs, Hungary; e-mail: dejozsi@gamma.ttk.pte.hu *(received: February 05, 2008; accepted: September 29, 2008).*

Key words: Hungary, China, Pliocene, red clay, palaeoenvironment, aeolian deposits.

INTRODUCTION

On the Chinese Loess Plateau, the Quaternary loess-palaeosol sequences are underlain by Tertiary red silty clay (Liu, 1985), termed the *Hipparion* Red-Earth (namely the "Red Clay"). The red clay in Hungary is also overlain by loess palaeosol sequences (Sümeghy, 1944; Jámbor, 1980, 1997; Halmai *et al*., 1982; Fekete *et al*., 1997; Schweitzer and Szöőr, 1997; Viczián, 2002; Kovács, 2003, 2008). The thickness of the red clay ranges from 10 to more than 100 m in China (Ding *et al*., 1998*a*, 1999; Sun *et al*., 1998; Guo *et al*., 2001; Lu *et al*., 2001; Hao and Guo, 2004, 2007; Li *et al.*, 2006; Xue *et al*., 2006) and from 4 to 90 m in Hungary (Jámbor, 1980, 1997; Halmai *et al*., 1982; Fekete *et al*., 1997; Schweitzer and Szöőr, 1997; Fekete, 2002; Földvári and Kovács-Pálffy, 2002; Viczián, 2002; Kovács, 2003, 2008). The Chinese deposit has been investigated for over 80 years (Anderson, 1923). The Hungarian red clays had been recognized earlier (Lóczy, 1886), but research on them was subsequently intermittent.

The remarkable progress made on red clay research worldwide show that the sedimentology, geochemistry, geomorphology and field relations all demonstrate a wind-blown origin for the Chinese red clay (Ding *et al*., 1998*a*,*b*; Lu *et al*., 2001; Xiong *et al*., 2002; Sun *et al*., 2002; Miao *et al*., 2004; Yang and Ding, 2004; Sun *et al*., 2006), similar to that for the overlying Pleistocene and Holocene loess.

In Hungary, little attention has been paid to the red clay over the last century. Different views on the formation, properties and distribution of red clays in Hungary have been published. Early scientists described the red clay as a variety of loess, sediment formed by the deposition of wind-blown silt (Lóczy, 1886; Sümeghy, 1944), while in the last decade there have been geological, mineralogical and pedological studies (Jámbor, 1997; Schweitzer and Szöőr, 1997; Fekete, 2002; Földvári and Kovács-Pálffy, 2002; Viczián, 2002). Studies of the geology, geomorphology, mineralogy and geochemistry have been carried out by only a few authors (Schweitzer and Szöőr, 1997; Kovács, 2003, 2007). Recent investigations also demonstrate an aeolian origin for the red clay in Hungary (Kovács, 2006, 2008). This paper presents results of grain-size, mineral and chemical analyses and their importance for the interpretation of the origin of the Quaternary deposits in Hungary and China. The aim of this study is to demonstrate the extent of similarities between the Chinese and Hungarian deposits, as well as show their importance in palaeoenvironmental research.

GEOLOGICAL SETTING

The Pliocene Upper Red-Earth Formation at Xifeng (Fig. 1) is well known from several research projects (Ding *et al*., 1998*a*,*b*; Sun *et al*., 1998, 2002; Lu *et al*., 2001; Xiong *et al*., 2002; Vandenberghe *et al*., 2004; Yang and Ding, 2004; Liu *et al*., 2006; Xue *et al*., 2006; Wang *et al*., 2006). Detailed geological and stratigraphical descriptions of the Upper Red-Earth at Xifeng can be found in Guo *et al*. (2001, 2004). In the eastern Loess Plateau region, the Red-Earth sequences generally have a silty-clay or clayey-silt texture, a hue varying from 7.5 to 5 YR, and contain abundant carbonate-rich layers (Guo *et al*., 2001). The Xifeng section (107°58'E, 35°53'N) is located in the central part of the Loess Plateau; the entire Red-Earth Formation in the region is generally 50–60 m thick and is a type sequence for the eastern Loess Plateau region (Liu, 1985; Sun *et al*., 1998; Guo *et al*., 2001; Lu *et al*., 2001). The Late Miocene–Pliocene Red Clay Formation of the Xifeng section overlies lacustrine strata and is overlain by Quaternary loess of the past 2.5 Ma. This unit of the Red-Earth section consists of alternating reddish layers (5 YR 5/6–8) and yellowish to brownish layers (7.5 YR 5/6–8). Each of the reddish layers are underlain by a carbonate-rich horizon. The reddish layers are characterized by disseminated, relatively soft calcareous nodules (10–20 cm in diameter).

The red clay deposits of the Carpathian Basin are known from both exposures and boreholes. The sections investigated in this study are located mainly in the foothills of the Hungarian mountains except for the central part (Fig. 2). The age of the Tengelic Red Clay Formation is ~3.5–1.0 Ma (Gyalog and Budai, 2004). For correlation with the neighbouring area see Table 1.

The underlying (Miocene–Lower Pliocene) strata are generally composed of thick greyish-yellow, mica-rich, cross-bedded sand and sandy clay or locally limestone (in Southern Hungary). In the northern part of the country, the lower part of the sand unit contains a variety of fossils (animals, plants), sometimes between sandstone benches. Many bone fragments, such as teeth, jaws, ribs of *Hipparion* sp., *Mastodon* sp., *Rhinoceros* sp. and *Sus* sp. can be found in the upper part of the sand bed (Kovács, 2003; Fábián *et al*., 2008). The age of the recovered vertebrate fossils is ~6 Ma (Fábián *et al*., 2008). The cross-bedded sand or sandy clay is overlain by a 3–20 m thick red clay unit (Fig. 3). The thickness of this unit is about 3 to 6 m in the northern and southern parts of the country (Fig. 3A, B). In the central part (especially in boreholes) this thickness is much greater (10–20 m or more). The red clay (5 YR 5/6) displays a

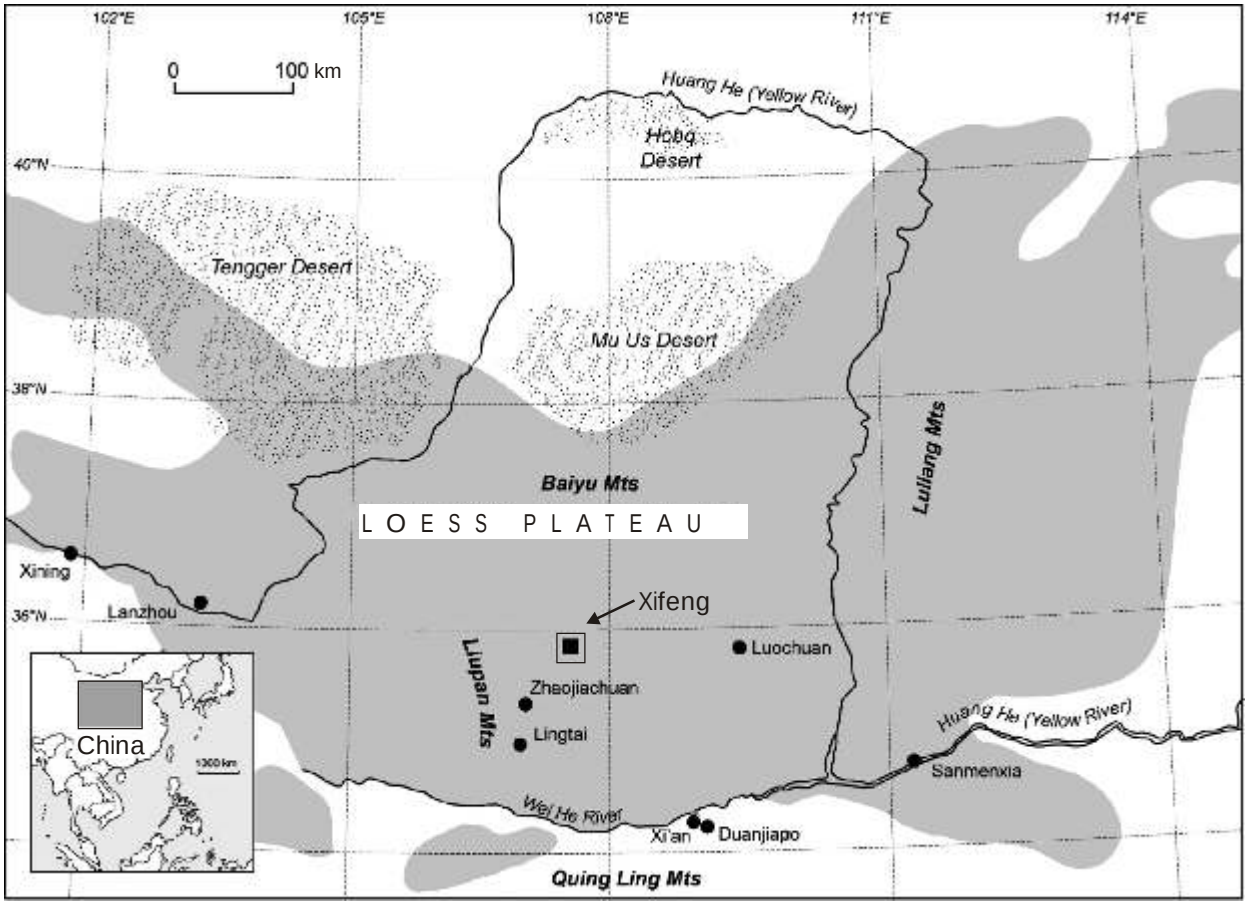

Fig. 1. Sketch map showing the location of the Xifeng profile in the Loess Plateau of China

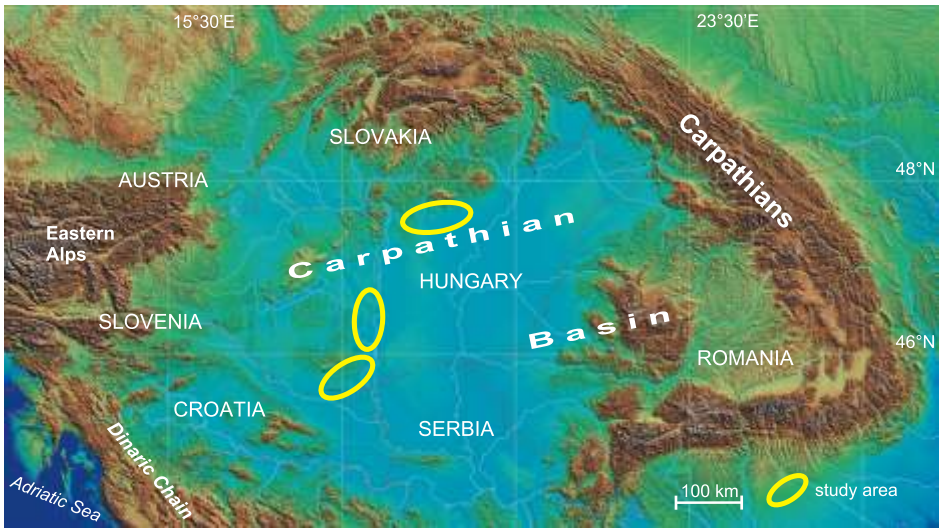

Fig. 2. Schematic map showing the study areas of the red clay deposits in Hungary (modified after Horváth and Bada, 2005)

Table 1

Correlation of the Pannonian Basin lithostratigraphy with neighbouring areas (after Piller *et al.*, 2004; Kováč *et al.*, 2006)

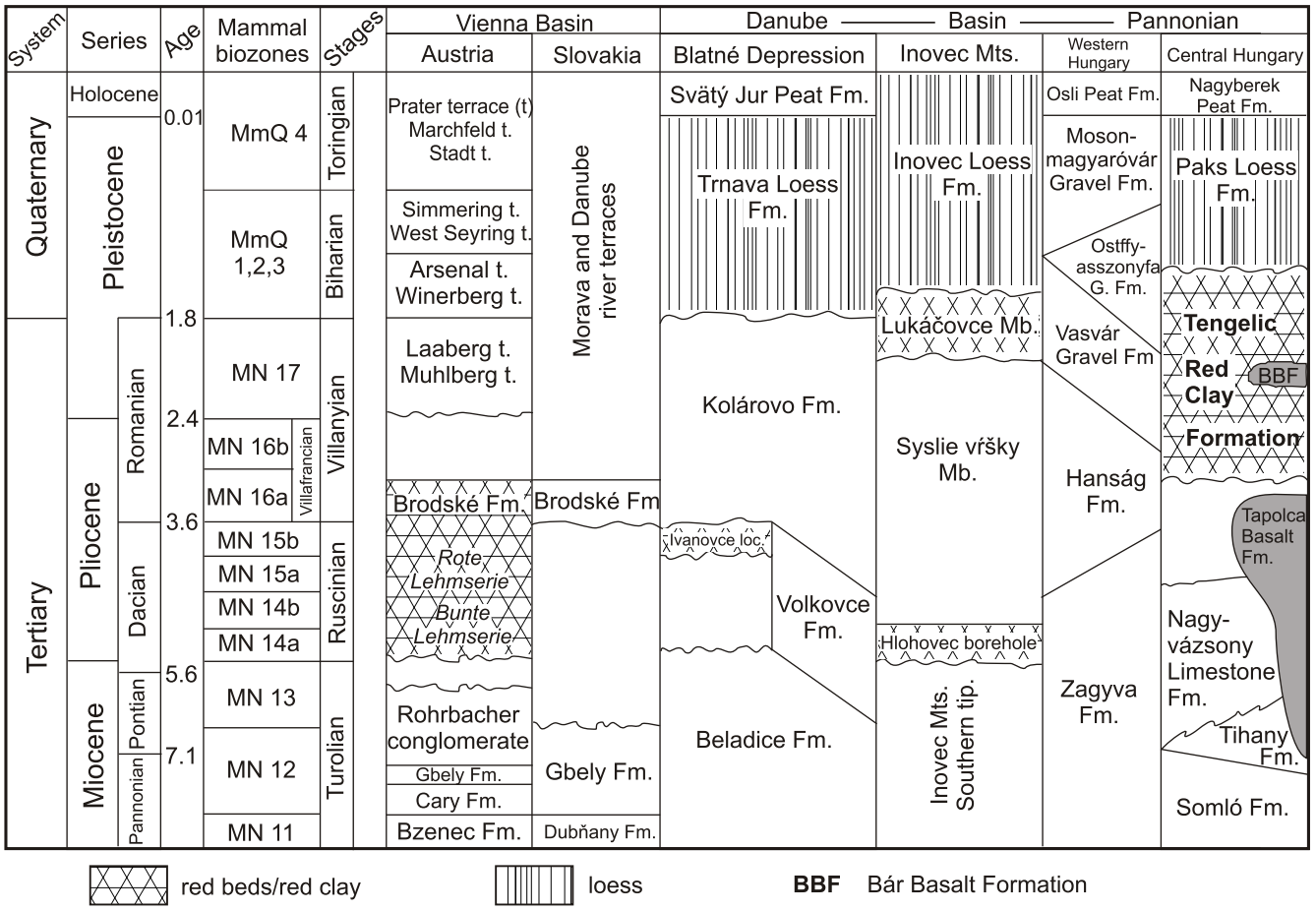

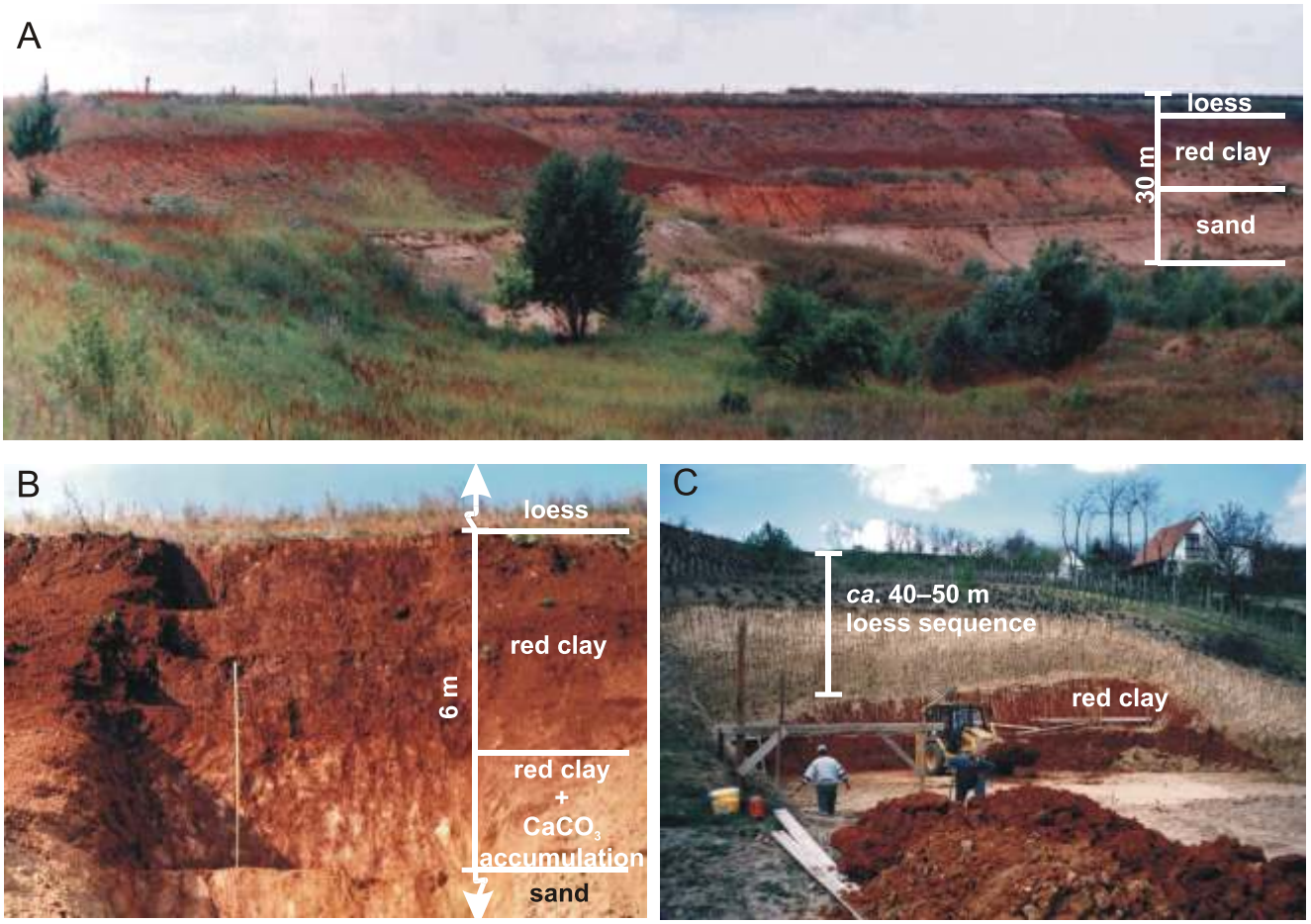

Fig. 3A — study site in Northern Hungary (Atkár); B — close-up profile of the red clay (Atkár); C — overlying loess sequence in Central Hungary (Szekszárd)

prismatic structure with slickensides, stress surfaces and brown and yellowish spots. $CaCO_3$ nodules, 3–5 cm in diameter, occur in the lower part of the red clay. Generally, the colour of the lower part is lighter than that of the upper part. Black Fe-Mn stains are generally abundant throughout the entire red clay unit, which is covered by the Quaternary loess-palaeosol succession (Fig. 3C).

MATERIALS AND METHODS

Red clay samples from the Pannonian Basin were collected during the fieldwork. A total of 50 samples were taken from the northern, southern and central parts of Hungary. The sequences were continuously sampled at 10–20 cm intervals. All samples were transferred to the laboratory for granulometric, chemical and mineralogical analyses. The grain-size distribution of all samples was measured by laser diffraction (*Fritsch Analysette 22*) methods according to the approach described by Konert and Vandenberghe (1997).

Subsamples for geochemical analysis were finely ground in an agate mill. Sediment powders (for AAS — Atomic Absorption Spetroscopy) of 1 g were then digested with 55 ml of concentrated nitrohydrochloric acid (aqua regia) and 10 ml 0.1 N HCl in an airtight Teflon crucible (Kovács, 2007). Concentrations of trace elements in the digested solutions were determined by a *Perkin Elmer AAnalyst 600*. Concentrations of major and trace elements were determined by a *Fisons Instruments ARL 8410* type sequential, wavelength-dispersive *XRF* spectrometer (equipped with a Rh-anode, 3-kW end-window X-ray tube) as described by Kovács (2007). Precision and accuracy were confirmed by replicate analyses of national standards (GSD-2 and GSD-6) and the use of blanks. Analytical uncertainties are generally less than 5%. Loss on ignition (LOI) was obtained by weighing after 1 hour of calcination at 950°C.

X-ray diffraction and thermal analysis (DTA) were applied to determine the mineral composition. Samples were measured with a *Philips* X-ray *Diffractometer* (*PW 1730 series*), using CuKα radiation and a *Paulik-Paulik-Erdey* type derivatograph.

The monomineralic quartz fraction of 50 samples from Hungary was extracted using the sodium pyrosulfate fusion–hydrofluorosilicic acid method (Xiao *et al.*, 1995). Scanning electronic microscopy (SEM) analyses were performed on the samples with a *JEOL JCM 5800*.

The average values of 50 Hungarian samples are represented by five points in Figures 4, 5 and 9 because of the correlation of five published Xifeng Upper Red-Earth data.

MICROMORPHOLOGY AND GRAIN-SIZE OF THE RED CLAY

Grain-size distributions of detrital deposits are usually regarded as useful parameters in characterizing sedimentary environments and dynamics. Grain-size distributions of the red clay were analysed and compared with those of typical aeolian loess and of the palaeosols developed on loess (Guo *et al*., 2001; Lu *et al*., 2001; Kovács, 2006, 2008). Lu *et al*. (2001) sedimentological data were used to present the grain-size parameters of the red clays. The granulometric results are presented in Table 2. The grain-size distribution curves of the Hungarian samples demonstrate a predominantly bimodal character (Fig. 4). The >63 μm (4φ) fraction is almost insignificant in the deposits. The fine fraction is clay or very fine silt, while the coarser fraction is medium to coarse silt. The modal size of the coarse fraction gradually coarsens from the Xifeng deposits (*ca*. 6–9φ) to the Hungarian red clay (5–7φ). Both red clay deposits show a bimodal character. In the Hungarian red clay, the coarser fraction is located between 4 and 6φ and the finer fraction between 7 and 9; in the Chinese red clay, these values are 4.5–6.5 and 8–10φ. The red clays are moderately sorted. Both deposits types show positively skewed to symmetric grain-size distribution. The positively skewed distribution indicates that the finer fraction is included in the grain-size distribution. We compare the statistical grain-size parameters of the Xifeng Red-Earth with the Tengelic Red Clay in Figure 5. Grain-size parameters vary a little, the characteristics of the Tengelic Formation being very similar to those of the Xifeng Red-Earth. Only the mean and skewness parameters are different, the mean square deviation (MSD) and kurtosis being almost identical.

SEM observations showed that the majority of the quartz grains from the Hungarian sites are finer than 100 μm in diameter, mostly ranging from 10 to 40 μm. Grains >60 μm represent a very small fraction. Most of the quartz grains have irregular and angular shapes (Fig. 6) and many are characterized by sharp edges, breaks and stepped surfaces (Fig. 6B, D), as well as conchoidal fractures (Fig. 6C). These grain-morphology fea-

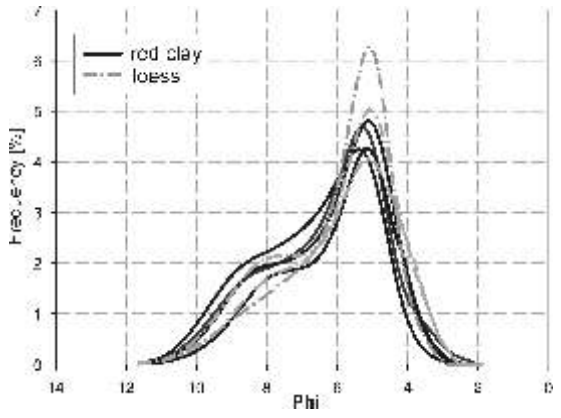

Fig. 4. Grain-size distribution curves of the Pliocene red clay and Quaternary loess samples from Hungary

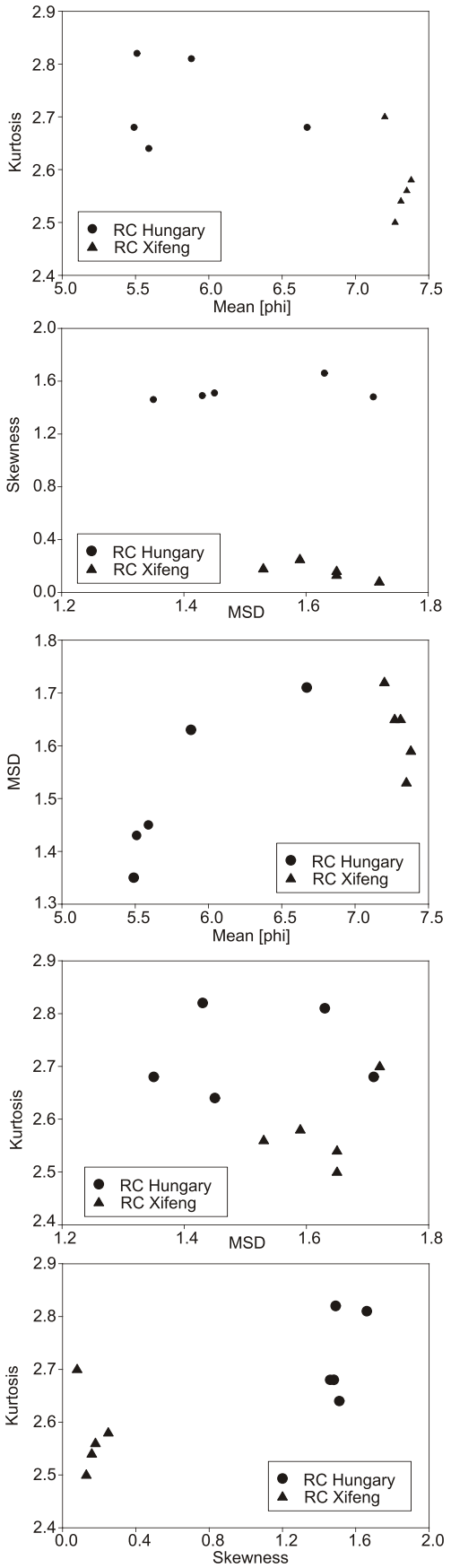

Fig. 5. Mean grain-size *vs*. sorting and skewness *vs*. kurtosis for fine grain samples in the Xifeng section and the Tengelic Red Clay

Table 2

Statistical parameters of grain-size distribution of the red clay deposits from Hungary and China

Sample	Mean	MSD	Skewness	Kurtosis
Hun-1	5.59	1.45	1.51	2.64
Hun-2	5.49	1.35	1.46	2.68
Hun-3	5.51	1.43	1.49	2.82
Hun-4	5.88	1.63	1.66	2.81
Hun-5	6.67	1.71	1.48	2.68
Xif-1	7.31	1.65	0.16	2.54
Xif-2	7.20	1.72	0.08	2.70
Xif-3	7.35	1.53	0.18	2.56
Xif-4	7.38	1.59	0.25	2.58
Xif-5	7.27	1.65	0.13	2.50

Hun-1 to Hun-5 — red clay samples from Hungary; Xif-1 to Xif-5 — red cley samples from China (data from Lu *et al*., 2001)

tures are very similar to those of the Xifeng aeolian samples (*cf*. fig. 1 in Liu *et al*., 2006; Guo *et al*., 2001, 2004), and also to those of Quaternary and Pliocene aeolian deposits elsewhere (Liu, 1985; Lu *et al*., 2001; Vandenberghe *et al*., 2004; Łącka *et al*., 2007; Kenig, 2008). They are considered characteristic of aeolian dust deposits (Pye and Sperling, 1983; Pye, 1995; Wright, 2001). The angular grains resulted from mechanical collisions, salt disintegration and freeze-thaw weathering in desert regions (Pye and Sperling, 1983; Wright, 2001, 2007; Smith *et al*., 2002), as aeolian dust in Northern China was mainly deflated from the northwestern desert lands (Liu, 1985; Ding *et al*., 1999). Because the dust grains were transported by wind in suspension, their sharp edges were not abraded. According to Pye and Sperling (1983), this kind of angular grain-morphology (Figs. 6 and 7C) is only characteristic of aeolian dust particles.

The structure of the red clay seen by optical microscopy are: an overall clayey texture (Fig. 7A), with few particles coarser than coarse silt (Fig. 7C); no oriented coatings are developed, but there are some weakly-arranged clay aggregates (Fig. 7B, D) and strips in channels and voids. Detrital calcium carbonate is rare, but there is a small quantity of weakly oriented micritic carbonate in channels and voids (Fig. 7D). There are a few scattered unoriented black-brown Fe-Mn stains (Fig. 7A). These characteristics show that the red clay is a type of palaeosol which developed in a semiarid environment (see later in Discussion and conclusions).

These sedimentological data are therefore highly consistent with the morphological features that support an aeolian origin for the Upper Red-Earth at Xifeng and for the red clay in the Carpathian Basin.

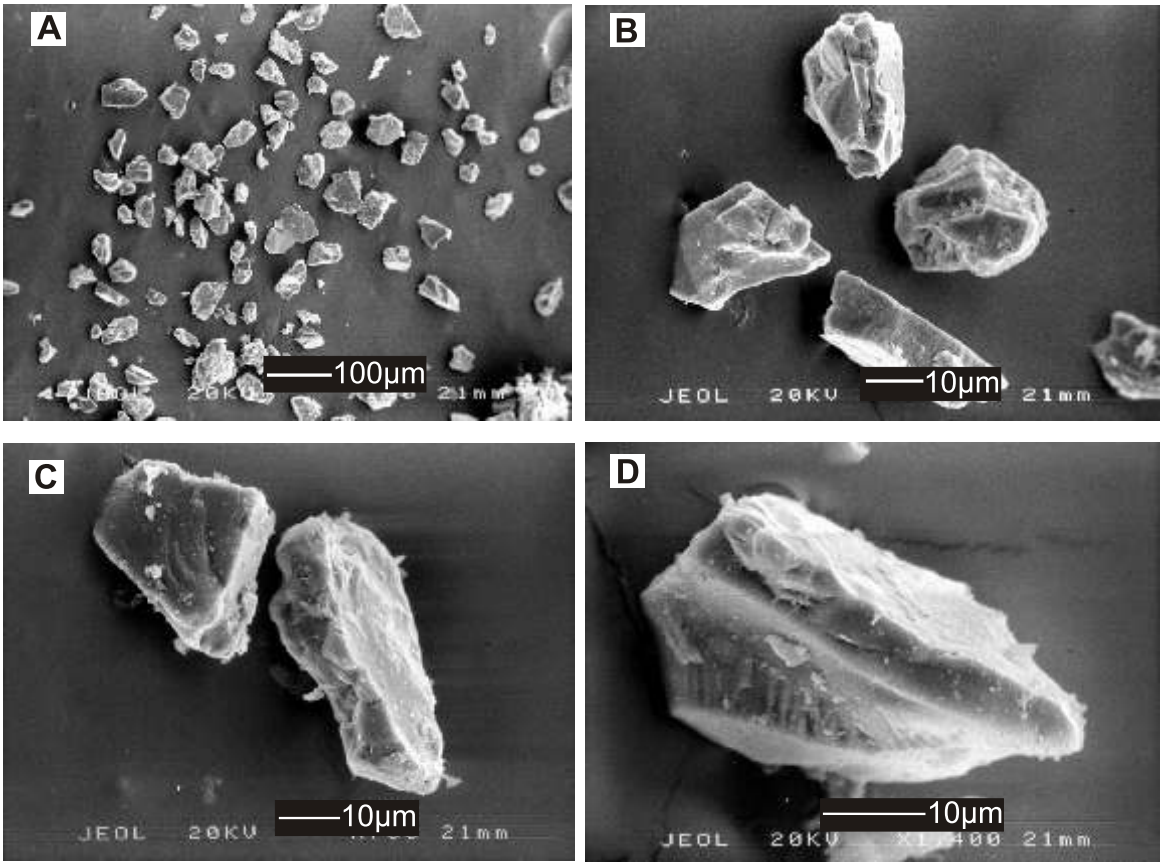

Fig. 6. Scanning electron microscopic photographs of <60 µm quartz grains from the Tengelic Red Clay (Hungary)

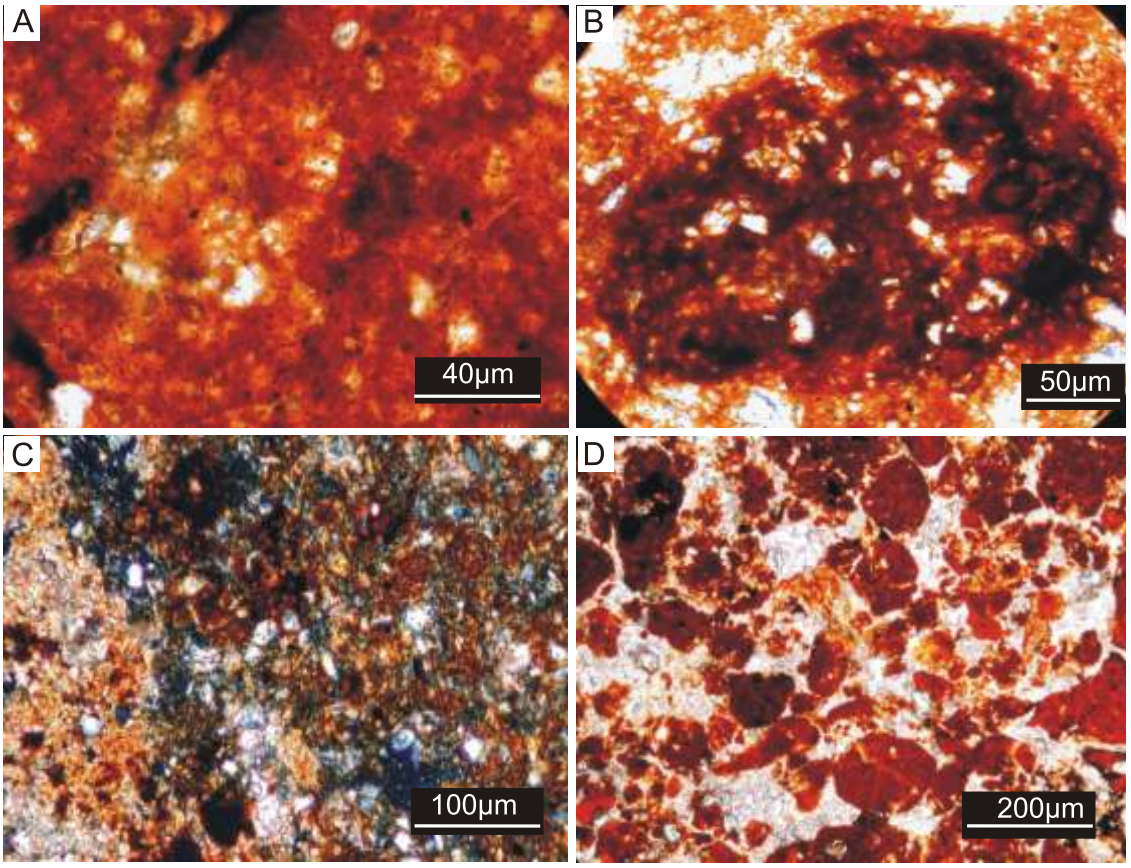

Fig. 7. Micromorphological features of the Tengelic Red Clay

A — black-brown Fe-Mn stains (natural light — NL); **B** — soil fragments in the red clay (NL);
C — angular morphology of the coarse grains in the red clay (polarized light — PL);
D — pedogenic carbonate and clay aggregations (NL)

MINERALOGY

Thin-section observations (Fig. 7C) show that (at both the Chinese and Hungarian sites) the coarse fraction (>10 μm) mainly consists of quartz (50–60%) and feldspar and micas (>30%). Pyroxene, hornblende, goethite and hematite were also observed. The mineralogy of the red clay was determined for the <2 μm size fraction (x-ray diffraction — XRD and differential thermal analysis — DTA). The major components are illite, kaolinite, quartz, plagioclase, smectite and chlorite with a high amount of amorphous matter (Schweitzer and Szöőr, 1997; Földvári and Kovács-Pálffy, 2002; Viczián, 2002; Kovács, 2007).

GEOCHEMICAL PROPERTIES OF THE RED CLAY DEPOSITS

MAJOR ELEMENTS

The chemical composition of the red clay deposits in Hungary is dominated by SiO_2, Al_2O_3, Fe_2O_3, CaO, MgO and K_2O, similar to that of the Xifeng Red-Earth (Table 3 and Fig. 8A). There are clear differences in loss on ignition (LOI) between the Hungarian and the Chinese deposits, which may result from differences in the content of carbonate, organic matter and hydrous phases (Table 3). After recalculation on a volatile-free basis, there is a high correlation (R^2 = 0.98) of major element concentration between the two red clay deposits (Fig. 8A).

The chemical index of alteration (CIA) for the samples varies from 67 to 80 (Fig. 9). In the (A–CN–K) triangular diagram (Fig. 9), insoluble residues lie close to the area of illite and smectite. The ternary diagram shows that all of the deposits lie parallel to the A–CN line. This pattern suggests that chemical weathering of the sediments resulted in removal of Ca and Na (primarily plagioclase) from the source rocks and less leaching of K, whereas in the sediments it caused considerable dissolution of Ca–Na host minerals and even K-bearing minerals (mainly K-feldspar) as well. The Chinese CIA values are around 70; those of the Hungarian deposits are closer to 80. These results show that chemical weathering was more intensive in Central Europe than in China.

TRACE ELEMENTS

We recalculated the trace element concentrations on a volatile-free basis (Table 4). Comparisons of the average concen-

Table 3

Major element composition of red clay samples from Hungary and China [wt.%]

Samples	SiO_2	TiO_2	Al_2O_3	Fe_2O_3	MnO	CaO	MgO	K_2O	Na_2O	P_2O_5	LOI
Hun-1	56.60	1.02	18.80	7.20	0.12	1.61	2.49	2.29	0.26	0.15	9.21
Hun-2	57.40	0.76	18.20	6.90	0.11	1.94	2.25	2.83	0.48	0.09	8.70
Hun-3	55.00	0.93	19.00	6.80	0.09	1.68	1.66	1.86	0.25	0.08	12.50
Hun-4	57.90	1.05	18.70	6.70	0.13	0.95	2.33	2.13	0.39	0.09	9.40
Hun-5	56.10	0.95	18.90	6.70	0.08	1.21	3.23	2.18	0.64	0.08	9.70
Xif-1	52.90	0.63	11.65	3.89	0.09	1.03	2.44	2.24	0.74	0.12	14.00
Xif-2	49.61	0.60	11.38	3.81	0.08	1.26	2.43	2.11	0.55	0.09	16.00
Xif-3	52.43	0.64	12.13	4.08	0.06	0.98	3.00	2.34	0.64	0.12	13.86
Xif-4	51.74	0.64	12.03	3.96	0.09	1.02	3.00	2.31	0.63	0.12	14.35

Xif-1 to Xif-4 — red clay samples from China (data from Guo *et al*., 2001, 2004); LOI — loss on ignition; for other explanations see Table 2

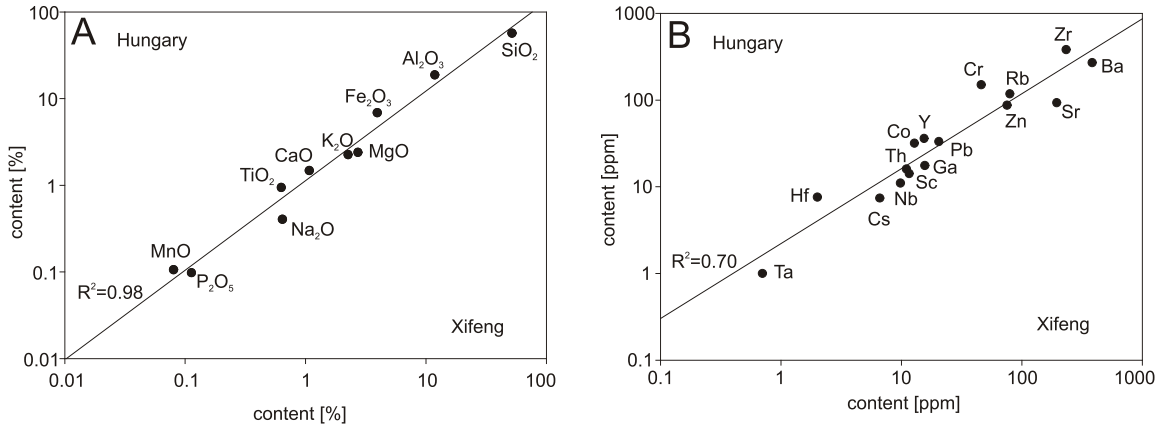

Fig. 8. Elemental composition of the red clay deposits from Hungary and China

A — comparison of major element composition between the red clay deposits;
B — comparison of trace element composition between the red clay deposits

trations of trace elements between the two red clay deposits are shown in Figure 8B. The strong similarity between the Chinese Red-Earth deposit and the Hungarian red clay again supports the conclusion that the Miocene Red-Earth deposit is of wind-blown origin, and that the Miocene Red-Earth deposit has a similar source provenance to that of the late Quaternary loess-soil in this region (Guo *et al*., 2001, 2004; Kovács, 2007, 2008). While the quantity of most of the trace elements in the Red-Earth deposit is comparable to those in the loess-soil units, some elements (e.g., Sr, Zr, Hf) are slightly depleted in the Red-Earth deposit (Ding *et al*., 2001; Guo *et al*., 2001, 2004; Kovács, 2007). This may be due to stronger chemical weathering, which is in agreement with field pedogenic observations, suggesting that the climate of the Middle Miocene in the north-eastern Tibetan Plateau area and the Middle Pliocene in the Carpathian Basin were warmer and wetter than during the Late Pleistocene.

An average upper continental crust (UCC)-normalized spiderdiagram for the samples from the Pliocene red clay sequences is shown in Figure 10. In the Hungarian samples, the in-

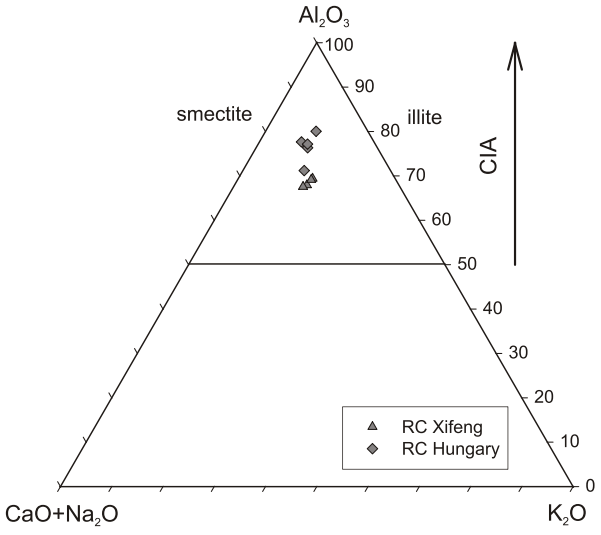

Fig. 9. The ternary diagrams showing the weathering trend of red clays (all in molar proportions); basic Al_2O_3–CaO+Na_2O–K_2O (A–CN–K) ternary diagram with CIA (chemical index of alteration) values

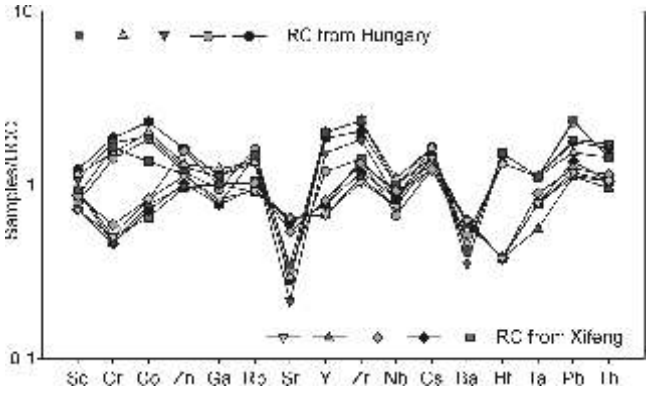

Fig. 10. UCC-normalized spiderdiagrams for samples from the red clay profiles of China and Hungary

soluble residues are characterized by remarkable depletion in Sr, Nb, Ba and enrichment in Cr and Co relative to UCC. Some elements (e.g., Cr, Co, Sr, Ba, Hf) are slightly depleted in the Xifeng samples. Comparing with the two red clay areas, only Cr, Co and Hf are different, the other elements being almost identical. Depletion of Sr is more related to feldspar weathering than to $CaCO_3$ dissolution. In sedimentary processes, the distribution of Sr is affected by strong adsorption on to clay minerals. Strontium is easily mobilized during weathering, especially in oxidising acid environments, and is incorporated into clay minerals.

DISCUSSION AND CONCLUSIONS

Sediment accumulation rates increased on or near continents in Late Cenozoic time, near 2–4 Ma. Obviously, such increases in sedimentation suggest increased rates of erosion of nearby terrain. Sources of sediment can be high or low terrain and tectonically active or inactive regions (Molnar, 2004). One of the preconditions for the formation of the aeolian sequences in China and Hungary is the existence of arid lands. Aridification in the dust source areas leads to vegetation degeneration, shrinking rivers and lakes, as well as to extensive areas of bare surface, which causes intensification of physical weathering and of wind abrasion. This will produce large quantities of silt (Wright, 2007).

CHINA

Two main factors may be invoked to explain desertification in the interior of Asia in the Late Miocene–Pliocene time. Climate models suggest that the uplift of the Tibetan Plateau may have played an important role in Asian aridification through modulating the atmospheric circulation and its barrier effect to moisture (Ruddiman and Kutzbach, 1989; Manabe and Broccoli, 1990; An *et al*., 2001; Guo *et al.*, 2002; Zhang *et al*., 2007). Another factor was the ongoing global cooling and the expansion of the Arctic ice-sheet, which is likely to have had a major impact on the intensity of the winter Siberian high pressure cell, resulting in higher continental aridity in Asia (Ruddiman and Kutzbach, 1989; Zhang *et al*., 2007).

CENTRAL EUROPE (CARPATHIAN BASIN)

Late Neogene changes in the palaeogeography and palaeotopography of Europe are mainly related to the African–Eurasian collision. These changes include the uplift of mountain ranges such as the Alps, Pyrenees, Carpathians and Caucasus, as well as the shrinking of the Paratethys Sea (Van Dam, 2006). Uplift within Europe explains further regional aridification and sharpening gradients, especially during the Pliocene. But the general consensus is that high topographies were not attained before Plio-Pleistocene times, implying that uplift might at least be held partly responsible for the ongoing aridification of parts of Central and Eastern Europe during the Pliocene. The shrinking of the Eastern Paratethys during the Early Pliocene (Dacian) to what are now the Caspian and Black Sea might additionally have explained aridification in that area (Popov *et al.*, 2006; van Dam, 2006).

The particle-size characteristics of the Neogene red clay deposits are very similar to those of the Pleistocene loess deposits (Fig. 4), suggesting an aeolian origin for the red clay (Kovács, 2006, 2007). It appears from the sedimentological data that the main part of the red clay is of wind-blown origins. What was the source of the red clay? Smith *et al*. (1991) has proposed local sources for loess and palaeosols in the Carpathian Basin. The Late Miocene deposits within the Carpathian Basin are loosely consolidated and underlie the Great Hungarian Plain. The Late Miocene deposits consist of marine and shallow lacustrine conglomerates, marls, sandstones, clays, and sands which were mainly eroded from the Eastern Alps (Magyar *et al*., 1999; Kuhlemann *et al*., 2002). Under suitably arid–semiarid conditions and/or limited vegetation cover, these sediments would provide a source of loose granular material, which could be entrained by aeolian processes (Kovács, 2003, 2008; Wright, 2007). The climate of the Early Pliocene was a transition between semi desert and savannah (Schweitzer and Szöőr, 1997; Kovács, 2003, 2008). Laboratory experiments have demonstrated the possibility that aeolian reworking of the Messinian sands and other similar deposits could theoretically have contributed material to the red clay, loess and loess-like deposits of the Carpathian Basin (Smith *et al*., 1991, 2002; Kovács, 2008). As a result, the red clay was transported by weak westerly winds and was then modified by post-depositional alteration (Fig. 11). This means that silty (loess-like) material was originally deposited and later it was weathered to red clay. The palaeoclimate of the Middle Pliocene (*ca*. 3 Ma) was generally warmer than at present, particularly at middle to high latitudes. The precipitation increase around 3 Ma, which just preceded the onset of the Late Pliocene–Pleistocene glacial–interglacial alternations, could be a reflection of the globally recognized “Mid-Pliocene warmth” (Van Dam, 2006). The effects of transgression accompanying the Pliocene optimum can explain the return to wetter conditions in Eastern Europe around 3 Ma. Farther continent-inward transport of Atlantic moisture as postulated by Haywood *et al*. (2000) could also have played a role. According to Haywood *et al*. (2000), in the European and Mediterranean region the climate was warmer (by 5°C), wetter (by 400–1000 mm/yr), and less seasonal than at present. The weathering values suggest that the Neogene palaeoclimate in the Carpathian Basin was more hu-

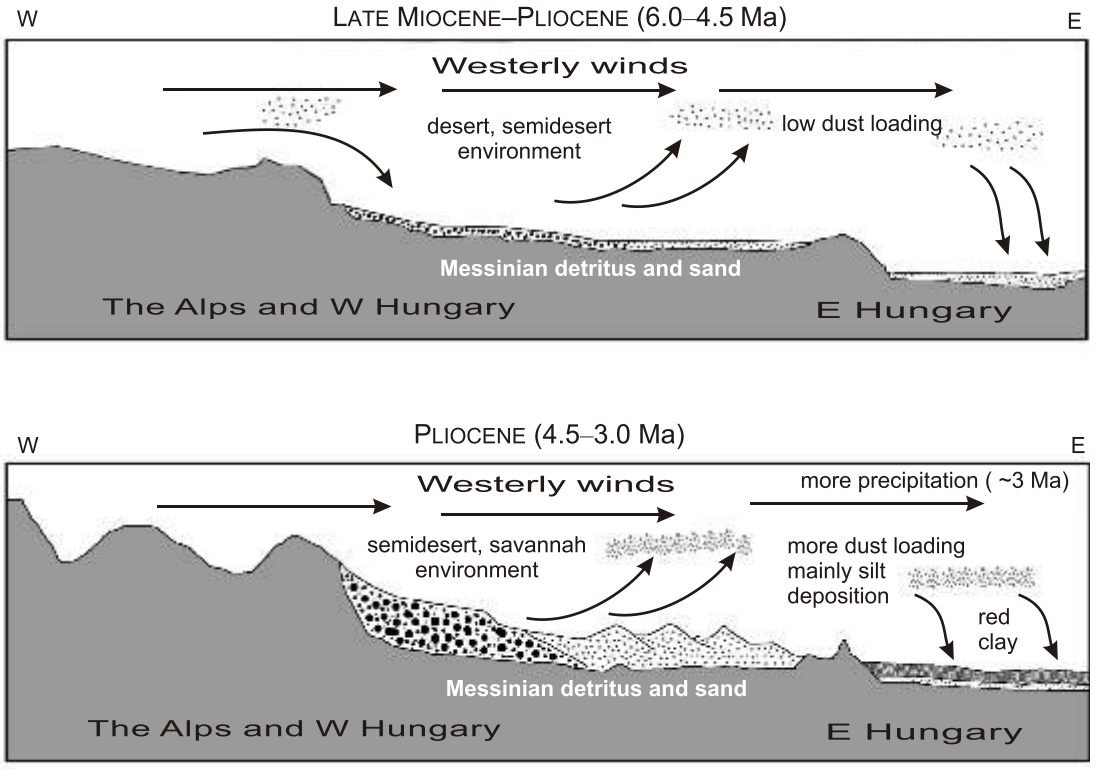

Fig. 11. Illustration of the hypothesized depositional processes of the red clay in the Carpathian Basin (Late Miocene and Pliocene)

mid and hotter (thus favouring intense chemical weathering) compared to the present climate regime with an average annual temperature of 10°C and precipitation of 500–700 mm. In the Pliocene (~3 Ma) the Carpathian Basin was situated in a warm and humid subtropic-kind zone with annual temperature and precipitation averaging 13–17°C and 800–1000 mm, or more (Jánossy, 1971; Montuire *et al*., 2006). Similar deposits (namely "red beds" or "Rote Lehm?" or "rubefied palaeosols?") to the Tengelic Red Clay can be found in the neighbouring area in the Vienna Basin and in Slovakia (e.g., Lukáčovce Member, Kováč *et al*., 2006) as well as in the northern foreland of the Carpathians (Grabowski, 2004; Ber, 2005; Lindner *et al.*, 2006). At present the origin of such "red" soils need conditions with average summer temperatures in the interval from 21 to 30°C and seasonal humidity only for a few months (*ca*. 4 months) in the year (Kováč *et al*., 2006).

The Neogene red clay accumulated under persistent weak winds and a rather steady warm-arid climate. The red clay, as well as the loess, thickens from west to east in the Carpathian Basin. Therefore, we infer that the clay-transporting wind came from the west, maybe from Central Europe, and we interpret these winds as driven by the westerlies. Modern dust observations and simulation experiments have suggested the coarse grain population or silt fractions in aeolian sediments, with an average grain-size range of >20 μm, could only be suspended for short intervals at low altitudes, even if entrained by strong winds. Thus, the >20 μm particles in red clay should have been transported by low-level winds (Guo *et al.*, 2002; Wen *et al.*, 2005). The upper westerlies have been active as a planetary circulation system in the middle latitudes of the northern hemisphere and generally transport the fine populations (grain-size less than 10 μm) or clay fraction in long-distance suspension, depositing dust in downwind areas far from the source regions. More detailed analyses of the spatial variation of grain-size distribution could help resolve the implications for depositional environment and palaeowind directions.

The red clay was modified by post-depositional weathering under warm-humid climate. These environmental characteristics accompanying the deposition and weathering of red clay are responsible particularly for the finer grain-size distributions and a lower dustfall rate than for the overlying loess. The red clay is an aeolian deposit that has been subjected to strong pedogenesis during a warm and moist climate punctuated by small-amplitude oscillations of cold and dry climate inferred from field investigations in Hungary (colour variations, abundance of clay coatings and carbonate nodules) as well as in China (Ding *et al.*, 1999, 2001). Red clay formed during periods of warmer and moister climate is redder, contains more clay coatings and fewer carbonate nodules. According to Kováč *et al*. (2006), the development of "rubefied palaeosols" (or red clays) is a result of seasonal variation in humidity. Its development needed chemical weathering and a warm climate with seasonal humidity changes for some 100 thousand to some million years. A most striking feature of the red clay sequences is the existence of many horizontal carbonate nodule horizons at both locations (Hungarian, Chinese). The thickness of these horizons ranges from 10 to over 100 cm (Ding *et al.*, 1999, 2001; Kovács, 2003, 2008). Most of the nodules are less than

Table 4

Trace element composition of red clay samples from Hungary and China [ppm]

Samples	Hun-1	Hun-2	Hun-3	Hun-4	Hun-5	Xif-1	Xif-2	Xif-3	Xif-4	Xif-5
Sc	17.0	11.0	15.0	16.0	12.0	13.0	10.0	12.0	13.0	10.0
Cr	170.0	130.0	160.0	140.0	150.0	46.0	42.0	54.0	42.0	46.0
Co	39.0	31.0	32.0	34.0	23.0	11.0	12.0	14.0	13.0	14.0
Zn	108.0	79.0	84.0	88.0	77.0	64.0	68.0	105.0	65.0	75.0
Ga	19.0	16.0	19.0	21.0	13.0	17.0	13.0	17.0	17.0	14.0
Rb	120.0	130.0	110.0	110.0	120.0	85.0	78.0	84.0	74.0	76.0
Sr	90.0	103.0	68.0	94.0	110.0	196.0	194.0	171.0	206.0	206.0
Y	39.0	25.0	32.0	42.0	42.0	16.0	16.0	17.0	14.0	14.0
Zr	390.0	270.0	350.0	450.0	450.0	270.0	228.0	256.0	211.0	200.0
Nb	12.0	8.0	10.0	13.0	12.0	10.0	10.0	11.0	9.0	9.0
Cs	8.0	6.0	8.0	8.0	7.0	7.0	6.0	6.0	7.0	7.0
Ba	260.0	320.0	220.0	290.0	260.0	383.0	385.0	392.0	370.0	387.0
Hf	8.0	7.0	8.0	7.0	8.0	2.0	2.0	2.0	2.0	2.0
Ta	1.0	1.0	1.0	1.0	1.0	0.7	0.7	0.8	0.5	0.7
Pb	30.0	39.0	31.0	26.0	40.0	19.0	23.0	21.0	19.0	20.0
Th	17.0	15.0	18.0	15.0	15.0	11.0	11.0	12.0	10.0	11.0

Xif-1 to Xif-5 — red clay samples from China (data from Guo *et al*., 2001, 2004); for other explanations see Table 2

10 cm in diameter. In general, red clays show a redder colour than that of the soils in the overlying Pleistocene loess. The materials have been subjected to relatively strong pedogenic processes, as indicated by the relative abundance of clay and Fe-Mn skins (Ding *et al.*, 1999, 2001; Guo *et al*., 2001, 2004; Liu *et al*., 2006). Obviously, these are pedological B horizons. A remarkable difference between the soil horizons of the red clay and loess sequences is that the pedogenic A horizons are generally lacking in the red clay sequence, whereas a complete A–B–C sequence is readily recognized in some of the palaeosols in the Pleistocene loess deposits (Ding *et al.*, 1999). Besides, the upper and lower boundaries of the B horizons in the red clay sequence are indistinct. In a pedological sense, the entire red clay sequence may be regarded as an extremely thick soil complex (Ding *et al.*, 1999). No laminations are seen in the entire red clay sequence. Therefore, the characteristics of the red clay mentioned above may be best explained by accretionary processes associated with the accumulation of wind-blown dust.

We conclude that the red clay in the Carpathian Basin is of wind-blown origin, and that it was subsequently affected by weathering processes in the Pliocene–Early Pleistocene.

Acknowledgements. Thanks are extended to Prof. Z. T. Guo (Institute of Geology and Geophysics, Chinese Academy of Sciences) for helpful discussions and the provision data on the Chinese red clay, to Drs. S. Á. Fábián and G. Varga (Department of Physical Geography, University of Pécs) for field assistance. Two anonymous reviewers are thanked for their constructive comments and suggestions. The authors are also grateful to F. Csirkés (University of Chicago) for language improvement.

REFERENCES

AN Z. S., KUTZBACH J. E., PRELL W. L. and PORTER S. C. (2001) — Evolution of Asian monsoons and phased uplift of the Himalaya–Tibetan Plateau since Late Miocene time. Nature, **411**: 62–66.

ANDERSON J. G. (1923) — Essays on the Cenozoic of northern China. Mem. Geol. Surv. China Ser. A, **3**: 1–152.

BER A. (2005) — Polish Pleistocene stratigraphy — a review of interglacial stratotypes. Neth. J. Geosc., **84**: 61–76.

DING Z. L., SUN J. M., LIU T. S., ZHU R. X., YANG S. L. and GUO B. (1998*a*) — Wind-blown origin of the Pliocene red clay formation in the Chinese Loess Plateau. Earth. Planet. Sc. Lett., **161**: 135–143.

DING Z. L., SUN J. M., YANG S. L. and LIU T. S. (1998*b*) — Preliminary magnetostratigraphy of a thick eolian red clay-loess sequence at Lingtai, the Chinese Loess Plateau. Geophys. Res. Lett., **25**: 1225–1228.

DING Z. L., SUN J. M., YANG S. L. and LIU T. S. (2001) — Geochemistry of the Pliocene red clay formation in the Chinese Loess Plateau and

implications for its origin, source provenance and palaeoclimatic change. Geochim. Cosmochim. Acta, **65**: 901–913.

DING Z. L., XIONG S. F., SUN J. M., YANG S. L., GU Z. Y. and LIU T. S. (1999) — Pedostratigraphy and palaeomagnetism of a ~7.0 Ma eolian loess — red clay sequence at Lingtai, Loess Plateau, northcentral China and the implications for palaeomonsoon evolution. Palaeogeogr. Palaeoclimatol. Palaeoecol., **152**: 49–66.

FÁBIÁN S. Á., KOVÁCS J. and VARGA G. (2008) — Az atkári késő-miocén csontleletről. Földr. Ért.

FEKETE J. (2002) — Physical and chemical features of red clays in Northern Hungary. Acta Geol. Hung., **45**: 231–246.

FEKETE J., STEFANOVITS P. and BIDLÓ G. (1997) — Comparative study of the mineral composition of red clays in Hungary. Acta Agron. Hung., **45**: 427–441.

FÖLDVÁRI M. and KOVÁCS-PÁLFFY P. (2002) — Mineralogical study of the Tengelic Formation and the loess complex of the Tolna Hegyhát and Morágy Hills areas (Hungary). Acta Geol. Hung., **45**: 247–263.

GRABOWSKI D. (2004) — Lithostratigraphy and genesis of Quaternary strata between Lanckorona and Myślenice in the Western Outer Carpathians. Geol. Quart., **48** (4): 351–370.

GUO Z. T., PENG S. Z., HAO Q. Z., BISCAYE P. E. and LIU T. S. (2001) — Origin of the Miocene–Pliocene Red-Earth Formation at Xifeng in Northern China and implications for paleoenvironments. Palaeogeogr. Palaeoclimatol. Palaeoecol., **170**: 11–26.

GUO Z. T., PENG S. Z., HAO Q. Z., BISCAYE P. E., AN Z. S. and LIU T. S. (2004) — Late Miocene–Pliocene development of Asian aridification as recorded in the Red-Earth Formation in northern China. Global Planet. Change, **41**: 135–145.

GUO Z. T., RUDDIMAN W. F., HAO Q. Z., WU H. B., QIAO Y. S., ZHU R. X., PENG S. Z., WEI J. J., YUAN B. Y. and LIU T. S. (2002) — Onset of Asian desertification by 22 Myr ago inferred from loess deposits in China. Nature, **416**: 159–163.

GYALOG L. and BUDAI T. (2004) — Proposal for new lithostratigraphic units of Hungary. Ann. Rep. Geol. Inst. Hung., **2002**: 195–232.

HALMAI J., JÁMBOR A., RAVASZ-BARANYAI L. and VETŐ I. (1982) — Geological results of the borehole Tengelic-2. Ann. Inst. Geol. Publ. Hung., **65**: 93–138.

HAO Q. Z. and GUO Z. T. (2004) — Magnetostratigraphy of a late Miocene-Pliocene loess-soil sequence in the western Loess Plateau in China. Geophys. Res. Lett., **31**: L09209.

HAO Q. Z. and GUO Z. T. (2007) — Magnetostratigraphy of an early-middle Miocene loess-soil sequence in the western Loess Plateau of China. Geophys. Res. Lett., **34**: L18305.

HAYWOOD A. M., SELLWOOD B. W. and VALDES P. J. (2000) — Regional warming: Pliocene (3 Ma) paleoclimate of Europe and the Mediterranean. Geology, **28**: 1063–1066.

HORVÁTH F. and BADA G. (2005) — Atlas of the present-day geodynamics of the Pannonian Basin: Euroconform maps with explanatory text. Dept. Geophys., Eötvös Univ., Budapest, 2005.

JÁMBOR Á. (1980) — A pannoniai képződmények rétegtanának alapvonatkozása. Ált. Földt. Szemle, **14**: 113–124.

JÁMBOR Á. (1997) — A Közép-Dunántúl fiatal kainozoos rétegtanának és fejlődéstörténetének néhány kérdése. Annu. Rep. Hung. Geol. Inst., **1996** (2): 191–202.

JÁNOSSY D. (1971) — Middle Pliocene microvertebrates Fauna from the Osztramos loc I (Northern Hungary). Ann. Hist-Nat. Mus. Nation. Hung., **64**: 27–52.

KENIG K. (2008) — Depositional environments of loesses from the Sandomierz section, SE Poland, based on lithological and SEM studies. Geol. Quart., **52** (2): 169–182.

KONERT M. and VANDENBERGHE J. (1997) — Comparison of laser grain-size analysis with pipette and sieve analysis: a solution for the underestimation of the clay fraction. Sedimentology, **44**: 523–535.

KOVÁČ M., BARÁTH I., FORDINÁL K., GRIGOROVICH A. S., HALÁSOVÁ E., HUDÁČKOVÁ N., JONIAK P., SABOL M., SLAMKOVÁ M., SLIVA L. and VOJTKO R. (2006) — Late Miocene to Early Pliocene sedimentary environments and climatic changes in the Alpine–Carpathian–Pannonian junction area: a case study from the Danube Basin northern margin (Slovakia). Palaeogeogr. Palaeoclimatol. Palaeoecol., **238**: 32–52.

KOVÁCS J. (2003) — Terrestrial red clays in the Carpathian Basin: a paleoenvironmental approach. Geomorphol. Slovaca, **3**: 86–89.

KOVÁCS J. (2006) — Wind-blown origin of the Neogene red clay in the Pannonian Basin. Geophys. Res. Abstr., **8**: 04182.

KOVÁCS J. (2007) — Chemical weathering intensity of the Late Cenozoic "red clay" deposits on the Carpathian Basin. Geochem. Int., **45**: 1056–1063.

KOVÁCS J. (2008) — Grain-size analysis of the Neogene red clay formation in the Pannonian Basin. Int. J. Earth Sc., **97**: 171–178.

KUHLEMANN J., FRISCH W., SZÉKELY B., DUNKL I. and KÁZMÉR M. (2002) — Post-collisional sediment budget history of the Alps: tectonic versus climatic control. Int. J. Earth Sc., **91**: 818–837.

LI F. J., WU N. Q. and ROUSSEAU D. D. (2006) — Preliminary study of mollusk fossils in the Qinan Miocene loess-soil sequence in western Chinese Loess Plateau. Sc. China Ser. D-Earth Sc., **49**: 724–730.

LINDNER L., BOGUTSKY A., GOZHIK P., MARKS L., ŁANCZONT M. and WOJTANOWICZ J. (2006) — Correlation of Pleistocene deposits in the area between the Baltic and Black Sea, Central Europe. Geol. Quart., **50** (1): 195–210.

LIU J. F., GUO Z. T., QIAO Y. S., HAO Q. Z. and YUAN B. Y. (2006) — Eolian origin of the Miocene loess-soil sequence at Qin'an, China: evidence of quartz morphology and quartz grain-size. Chin. Sc. Bull., **51**: 117–120.

LIU T. S. (1985) — Loess and the Environment. China Ocean Press. Beijing.

LÓCZY L. (1886) — Report of the detailed geological survey in 1886. Ann. Rep. Geol. Inst. Hung., **1886**: 1–115.

LU H. Y., VANDENBERGHE J. and AN Z. S. (2001) — Aeolian origin and palaeoclimatic implications of the "Red Clay" (north China) as evidenced by grain-size distribution. J. Quat. Sc., **16**: 89–97.

ŁĄCKA B., ŁANCZONT M., MADEYSKA T. and BOGUCKYJ A. (2007) — Geochemical composition of Vistulian loess and micromorphology of interstadial palaeosols at the Kolodiiv site (East Carpathian Foreland, Ukraine). Geol. Quart., **51** (2): 127–146.

MAGYAR I., GEARY G. H. and MÜLLER P. (1999) — Paleogeographic evolution of the Late Miocene Lake Pannon in Central Europe. Palaeogeogr. Palaeoclimatol. Palaeoecol., **147**: 151–167.

MANABE S. and BROCCOLI A. J. (1990) — Mountains and arid climate of middle latitudes. Science, **247**: 192–195.

MOLNAR P. (2004) — Late Cenozoic increase in accumulation rates of terrestrial sediment: how might climate change have affected erosion rates? Ann. Rev. Earth Planet. Sc., **32**: 67–89.

MIAO X. D., SUN Y. B., LU H. Y. and MASON J. A. (2004) — Spatial pattern of grain size in the Late Pliocene "Red Clay" deposits (North China) indicates transport by low-level northerly winds. Palaeogeogr. Palaeoclimatol. Palaeoecol., **206**: 149–155.

MONTUIRE S., MARIDET O. and LEGENDRE S. (2006) — Late Miocene–Early Pliocene temperature estimates in Europe using rodents. Palaeogeogr. Palaeoclimatol. Palaeoecol., **238**: 247–262.

PILLER W. E., EGGER H., ERHART C. W., GROSS M., HATZHAUSER M., HUBMANN B., VAN HAUSEN D., KRENMAYR H.-G., KRYSTYN L., LEIN R., LUKENDER A., MANDL G. W., RÖGL F., ROETZEL R., RUPP C., SCHNABEL W., SCHÖNLAUB H. P., SUMMESBERGER H., WAGREICH M. and WESSELY G. (2004) — Die stratigraphische Tabelle von Österreich 2004 (sedimentre Schichtfolgen).

POPOV S. V., SHCHERBA I. G., ILYINA L. B., NEVESSKAYA L. A., PARAMONOVA N. P., KHONDKARIAN S. O. and MAGYAR I. (2006) — Late Miocene to Pliocene palaeogeography of the Paratethys and its relation to the Mediterranean. Palaeogeogr. Palaeoclimatol. Palaeoecol., **238**: 91–106.

PYE K. (1995) — The nature, origin and accumulation of loess. Quat. Sc. Rev., **14**: 653–667.

PYE K. and SPERLING C. H. B. (1983) — Experimental investigation of silt formation by static breakage processes: the effect of temperature, moisture and salt on quartz dune sand and granitic regolith. Sedimentology, **30**: 49–62.

RUDDIMAN W. F. and KUTZBACH J. E. (1989) — Forcing of late Cenozoic northern hemisphere climate by plateau uplift in southern Asia and the American West. J. Geophys. Res., **94**: 18409–18427.

SCHWEITZER F. and SZÖŐR G. (1997) — Geomorphological and stratigraphical significance of Pliocene red clay in Hungary. Z. Geomorphol. Suppl., **110**: 95–105.

SMITH B. J., WRIGHT J. S. and WALLEY W. B. (2002) — Sources of non-glacial loess-size quartz silt and the origins of "desert loess". Earth Sc. Rev., **59**: 1–26.

SMITH B. J., WRIGHT J. S. and WHALLEY W. B. (1991) — Simulated aeolian abrasion of Pannonian sands and its implications for the origins of Hungarian loess. Earth Surf. Proc. Land., **16**: 745–752.

SÜMEGHY J. (1944) — The territory east of the Tisza River (in Hungarian). Bull. Geol. Inst. Hung., **6**: 1–208.

SUN D. H., BLOEMENDAL J., REA D. K., VANDENBERGHE J., JIANG F. C., AN Z. S. and SU R. X. (2002) — Grain-size distribution function of polymodal sediments in hydraulic and aeolian environments, and numerical partitioning of the sedimentary components. Sed. Geol., **152**: 263–277.

SUN D. H., SHAW J., AN Z. S., CHENG M. Y. and YUE L. P. (1998) — Magnetostratigraphy and paleo-climatic interpretation of a continuous 7.2 Ma Late Cenozoic eolian sediments from the Chinese Loess Plateau. Geophys. Res. Lett., **25**: 85–88.

SUN Y. B., LU H. Y. and AN Z. S. (2006) — Grain size of loess, palaeosol and Red Clay deposits on the Chinese Loess Plateau: significance for understanding pedogenic alteration and palaeomonsoon evolution. Palaeogeogr. Palaeoclimatol. Palaeoecol., **241**: 129–138.

Van DAM J. A. (2006) — Geographic and temporal patterns in the late Neogene (12–3 Ma) aridification of Europe: the use of small mammals as paleoprecipitation proxies. Palaeogeogr. Palaeoclimatol. Palaeoecol., **238**: 190–218.

VANDENBERGHE J., LU H. Y., SUN D. H., VAN HUISSTEDEN J. and KONERT M. (2004) — The late Miocene and Pliocene climate in East Asia as recorded by grain size and magnetic susceptibility of the Red Clay deposits (Chinese Loess Plateau). Palaeogeogr. Palaeoclimatol. Palaeoecol., **204**: 239–255.

VICZIÁN I. (2002) — Typical clay mineral associations from geological formations in Hungary: a review of recent investigations. Geol. Carpath., **53**: 65–69.

WEN L. J., LU H. Y. and QUIANG X. (2005) — Changes in grain-size and sedimentation rate of the Neogene Red Clay deposits along the Chinese Loess Plateau and implications for the palaeowind system. Sc. China Ser. D-Earth Sc., **48**: 1452–1462.

WANG L., LÜ H. Y., WU N. Q., LI J., PEI Y. P., TONG G. B. and PENG S. Z. (2006) — Palynological evidence for Late Miocene–Pliocene vegetation evolution recorded in the red clay sequence of the central Chinese Loess Plateau and implication for palaeoenvironmental change. Palaeogeogr. Palaeoclimatol. Palaeoecol., **241**: 118–128.

WRIGHT J. S. (2001) — "Desert" loess versus "glacial" loess: quartz silt formation, source areas and sediment pathways in the formation of loess deposits. Geomorphology, **36**: 231–256.

WRIGHT J. S. (2007) — An overview of the role of weathering in the production of quartz silt. Sed. Geol., **202**: 337–351.

XIAO J. L., PORTER S. C., AN Z. S., KUMAI H. S. and YOSHIKAWA S. (1995) — Grain size of quartz as an indicator of winter monsoon strength on the Loess Plateau of central China during the last 130 000 year. Quat. Res., **43**: 22–29

XIONG S. F., SUN D. H. and DING Z. L. (2002) — Aeolian origin of the red earth in southeast China. J. Quat. Sc., **17**: 181–191.

XUE X. X., ZHANG Y. X. and YUE L. P. (2006) — Paleoenvironments indicated by the fossil mammalian assemblages from red clay-loess sequence in the Chinese Loess Plateau since 8.0 Ma B.P. Sc. China Ser. D-Earth Sc., **49**: 518–530.

YANG S. Y. and DING Z. L. (2004) — Comparison of particle size characteristics of the Tertiary "red clay" and Pleistocene loess in the Chinese Loess Plateau: implications for origin and sources of the "red clay". Sedimentology, **51**: 77–93.

ZHANG Z. S., WANG H. J., GUO Z. T. and JIANG D. B. (2007) — Impacts of tectonic changes on the reorganization of the Cenozoic paleoclimatic patterns in China. Earth Planet. Sc. Lett., **257**: 622–634.